Supporting Information

Chien *et al.* 10.1073/pnas.0811902106

SI Methods

Immunohistochemistry and Immunoblot Studies. A polyclonal rabbit anti–ß-catenin antibody (Sigma) was used for detection of β-catenin (1:1000 dilution for immunoblot, 1:200 dilution for immunohistochemistry). Cells were grown on 18-mm glass coverslips for 48–72 h, fixed using 4% paraformaldahyde, permeabilized using 0.25% Triton X-100, and then blocked with 10% goat serum. Goat anti-rabbit Alexa Fluor-568 antibody (Molecular Probes) was diluted 1:1000. Cells were counterstained for nucleic acid with DAPI (Molecular Probes). Cellular lysates were obtained by lysing cells on plate with a 0.1% Nonidet P-40–based buffer and analyzed by NuPage 4%–12% gradient gels (Invitrogen). The antibody used to confirm *WNT5A* expression was obtained from Cell Signaling Technologies.

Tumor Microarray Staining and Analysis. The tumor microarray used for this study is part of a larger previously published data set (1). For this study, we recruited tumor samples that had measured values by AQUA for ß-catenin, α-catenin, and Ki67, and also data on Breslow depth at diagnosis; any samples missing any of these measurements were excluded a priori from the analysis. Target antibodies were α-catenin, mouse monoclonal clone CAT-7A4 (Zymed) 1:150, and ß-catenin, mouse monoclonal clone 14 (BD Transduction Laboratories) 1:2500. Primary antibodies were incubated at 4 °C overnight. These antibodies have been validated previously (1). The secondary antibodies, Alexa 488–conjugated goat anti-rabbit (1:100; Molecular Probes) diluted into Envision anti-mouse (neat; DAKO), were applied for 1 h at room temperature. To visualize the nuclei, DAPI (1:100) was included with the secondary antibodies. Finally, a 10-min Cy5-tyramide (Perkin-Elmer Life Sciences) incubation labeled the target. Additional negative controls were obtained by omitting the target protein primary antibody. AQUA was performed as described previously (2). Target antigen expression levels were determined in an automated fashion, blinded to any clinical information. Statistical analyses, including Kaplan-Meier survival probabilities, ANOVA, and *t*-tests, were performed using the GraphPad Prism software package.

Genome-Wide Transcriptional Profiling with Agilent Microarrays and PCR Validation. Cells were cultured for ≈72 h until they reached 80%–90% confluency. RNA was purified using the RNeasy kit (Qiagen), following the manufacturer's protocol. cDNA was synthesized using SuperScript Reverse Transcriptase (Invitrogen). A Light Cycler FastStart DNA Master SYBR Green1 unit (Roche) was used for RT-PCR, as described previously (3). The qRT-PCR results presented in the text are representative of experiments performed on a minimum of 3 biological replicates.

Agilent whole mouse genome array analysis was performed at the microarray core facility of the Huntsman Cancer Institute, Salt Lake City, Utah. Data analysis, including *t*-tests (4), was performed using the TM4 microarray software suite, which is freely available online (5). Two-channel hybridizations were performed with labeled cDNA isolated from 3 biological replicates each for cells expressing either *WNT3A* or *WNT5A*, with cDNA from *GFP*-expressing cells used as the reference sample. These studies revealed gene sets regulated in both *WNT3A* and *WNT5A* cells, and the analysis and complete data sets are presented in supporting information (SI) Text. A list of published Wnt target genes is available at the Wnt homepage (http://www.stanford.edu/~rnusse/pathways/targets.html).

Discussion

Detection and Interpretation of Nuclear ß-Catenin in Melanoma Tumors. Previous studies using nuclear ß-catenin as a surrogate marker of Wnt/ß-catenin activation in melanoma (6–8) have relied on subjective manual scoring of histological samples rather than on the automated measurements described in this report. This type of histological scoring is invariably difficult to quantify, because it often fails to completely convey the variability of nuclear ß-catenin staining seen in tumors in terms of the number of positive cells and the relative levels between cells with positive staining. Nevertheless, findings from those studies support our finding that increased nuclear ß-catenin expression predicts improved patient outcome. Two other previous studies focused on ß-catenin in melanoma merit additional discussion (9, 10). These 2 studies involve overlapping patient cohorts with the current study, as mentioned in *Methods*. The study by Kreizenbeck *et al.* (9) also used AQUA to measure total levels of cellular ß-catenin but did not focus on subcellular distribution of ß-catenin as we did in the current analysis, nor did it correlate levels of ß-catenin to Ki-67.

The study by Kielhorn *et al.* (10) correlated the presence of (Ser-33/Ser-37/Thr-41)-phosphorylated nuclear ß-catenin (referred to subsequently as phospho-ß-catenin) with decreased survival in patients with melanoma. The finding of phospho-ß-catenin in the nucleus is itself somewhat paradoxical (as those authors acknowledged), because phosphorylation targets ß-catenin for proteasomal degradation. Some cases with phospho-ß-catenin staining exhibited minimal staining with the general ß-catenin antibody at the optimal titer, suggesting that phospho-ß-catenin comprises a small fraction of total ß-catenin, and possibly reflecting an increased affinity of the phospho-ß-catenin antibody (10). The authors speculated that the detection of nuclear phospho-ß-catenin may reflect alterations in the proteasomal pathway, which is interesting given that the presence of nuclear phospho-ß-catenin antibody also is correlated with improved patient prognosis in the setting of colorectal cancer, where activation of Wnt/ß-catenin signaling is seen in the majority of tumors (11). Given that proteins involved in regulating the degradation of phosphorylated ß-catenin also are found in nuclear pools [reviewed in ref. (12)], it is conceivable that the nuclear phospho-ß-catenin seen in tumors represents a small fraction of the total nuclear ß-catenin that is targeted for proteasomal degradation rather than for active signaling. Together, these findings suggest that the presence of nuclear phospho-ß-catenin may not necessarily function as a surrogate indicator of active Wnt/ß-catenin signaling.

1. Kreizenbeck GM, Berger AJ, Subtil A, Rimm DL, Gould Rothberg BE (2008) Prognostic significance of cadherin-based adhesion molecules in cutaneous malignant melanoma. *Cancer Epidemiol Biomarkers Prev* 17:949–958.
2. Camp RL, Chung GG, Rimm DL (2002) Automated subcellular localization and quantification of protein expression in tissue microarrays. *Nat Med* 8:1323–1327.
3. Major MB, *et al.* (2007) Wilms tumor suppressor WTX negatively regulates WNT/beta-catenin signaling. *Science* 316:1043–1046.
4. Pan W (2002) A comparative review of statistical methods for discovering differentially expressed genes in replicated microarray experiments. *Bioinformatics* 18:546–554.
5. Saeed AI, *et al.* (2003) TM4: A free, open-source system for microarray data management and analysis. *Biotechniques* 34:374–378.
6. Bachmann IM, Straume O, Puntervoll HE, Kalvenes MB, Akslen LA (2005) Importance of P-cadherin, beta-catenin, and Wnt5a/frizzled for progression of melanocytic tumors and prognosis in cutaneous melanoma. *Clin Cancer Res* 11:8606–8614.

7. Kageshita T, *et al.* (2001) Loss of beta-catenin expression associated with disease progression in malignant melanoma. *Br J Dermatol* 145:210–216.
8. Maelandsmo GM, Holm R, Nesland JM, Fodstad O, Florenes VA (2003) Reduced beta-catenin expression in the cytoplasm of advanced-stage superficial spreading malignant melanoma. *Clin Cancer Res* 9:3383–3388.
9. Kreizenbeck GM, Berger AJ, Subtil A, Rimm DL, Gould Rothberg BE (2008) Prognostic significance of cadherin-based adhesion molecules in cutaneous malignant melanoma. *Cancer Epidemiol Biomarkers Prev* 17:949–958.
10. Kielhorn E, *et al.* (2003) Tissue microarray–based analysis shows phospho-beta-catenin expression in malignant melanoma is associated with poor outcome. *Int J Cancer* 103:652–656.
11. Chung GG, *et al.* (2001) Tissue microarray analysis of beta-catenin in colorectal cancer shows nuclear phospho-beta-catenin is associated with a better prognosis. *Clin Cancer Res* 7:4013–4020.
12. Willert K, Jones KA (2006) Wnt signaling: Is the party in the nucleus? *Genes Dev* 20:1394–1404.
13. Barrett T, *et al.* (2007) NCBI GEO: Mining tens of millions of expression profiles–database and tools update. *Nucleic Acids Res* 35:D760–D765.
14. Talantov T, *et al.* (2005) Novel genes associated with malignant melanoma but not benign melanocytic lesions. *Clin Cancer Res* 11:7234–7242.
15. Smith AP, Hoek K, Becker D (2005) Whole-genome expression profiling of the melanoma progression pathway reveals marked molecular differences between nevi/melanoma in situ and advanced-stage melanomas. *Cancer Biol Ther* 4:1018–1029.

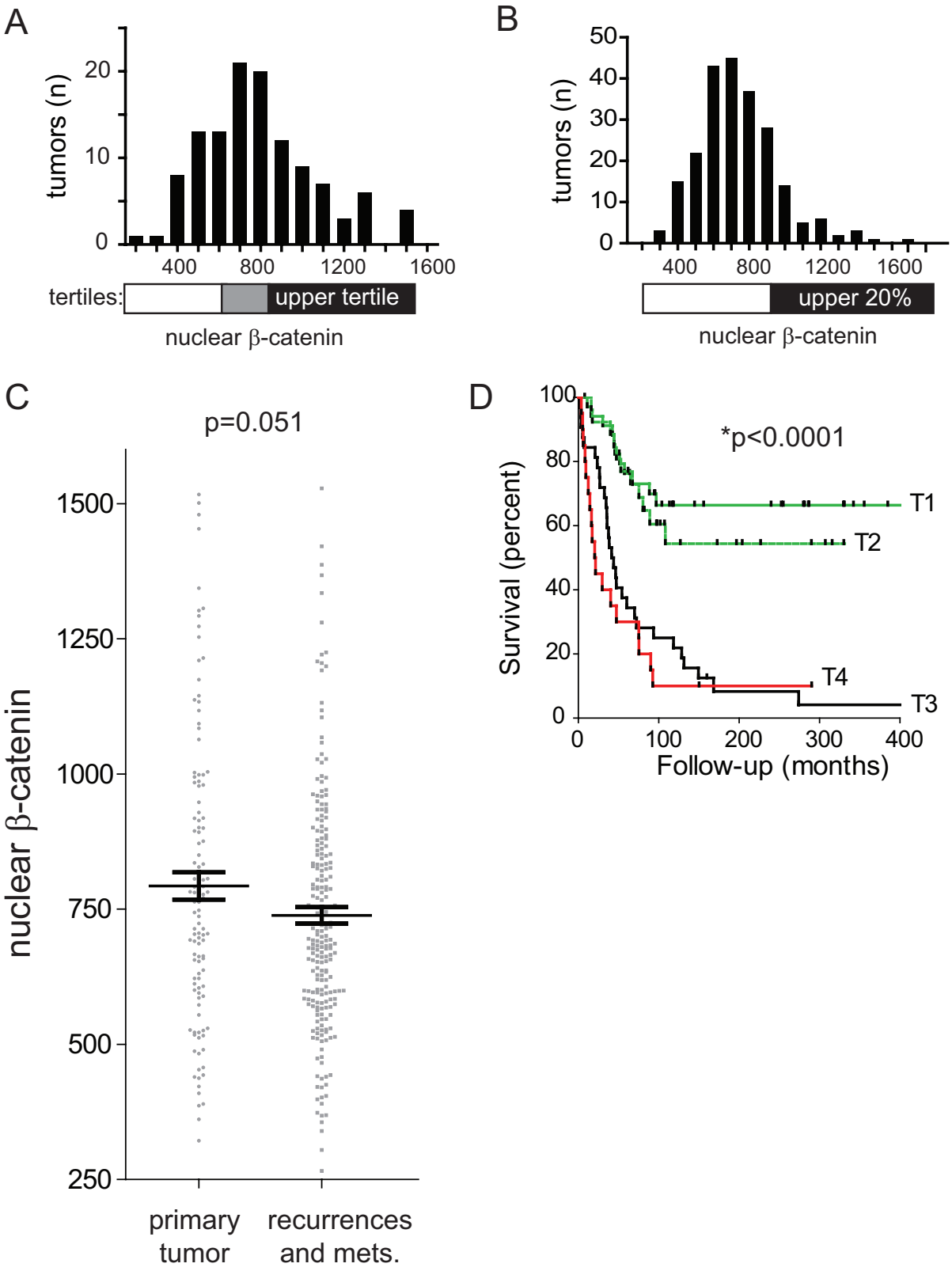

Fig. S1. Additional analysis of tumor microarray dataset. (*A*) A bar histogram binned by nuclear ß-catenin level showing the distribution within primary tumors ($n = 118$) and within the tertiles used to stratify tumors. This stratification was performed a priori based on the near-Gaussian distribution of tumors with varying nuclear ß-catenin levels. (*B*) For survival analysis, we stratified nuclear ß-catenin in recurrences and metastases by grouping the top 20% of tumors by nuclear ß-catenin level, which corresponds to the same levels seen in the upper tertile of primary tumors. (*C*) Bars show the average and SEM of nuclear ß-catenin levels in primary and metastatic/recurrent melanoma tumors. Gray dots represent individual tumors. The lower nuclear ß-catenin levels seen in metastases/recurrences compared with primary tumors approached, but did not meet, our criteria for statistical significance based on unpaired 2-tailed *t*-tests. (*D*) When tumors were stratified by AJCC staging criteria for tumor depth, Kaplan-Meier analysis revealed a significant survival trend (by log-rank test) based on Breslow thickness.

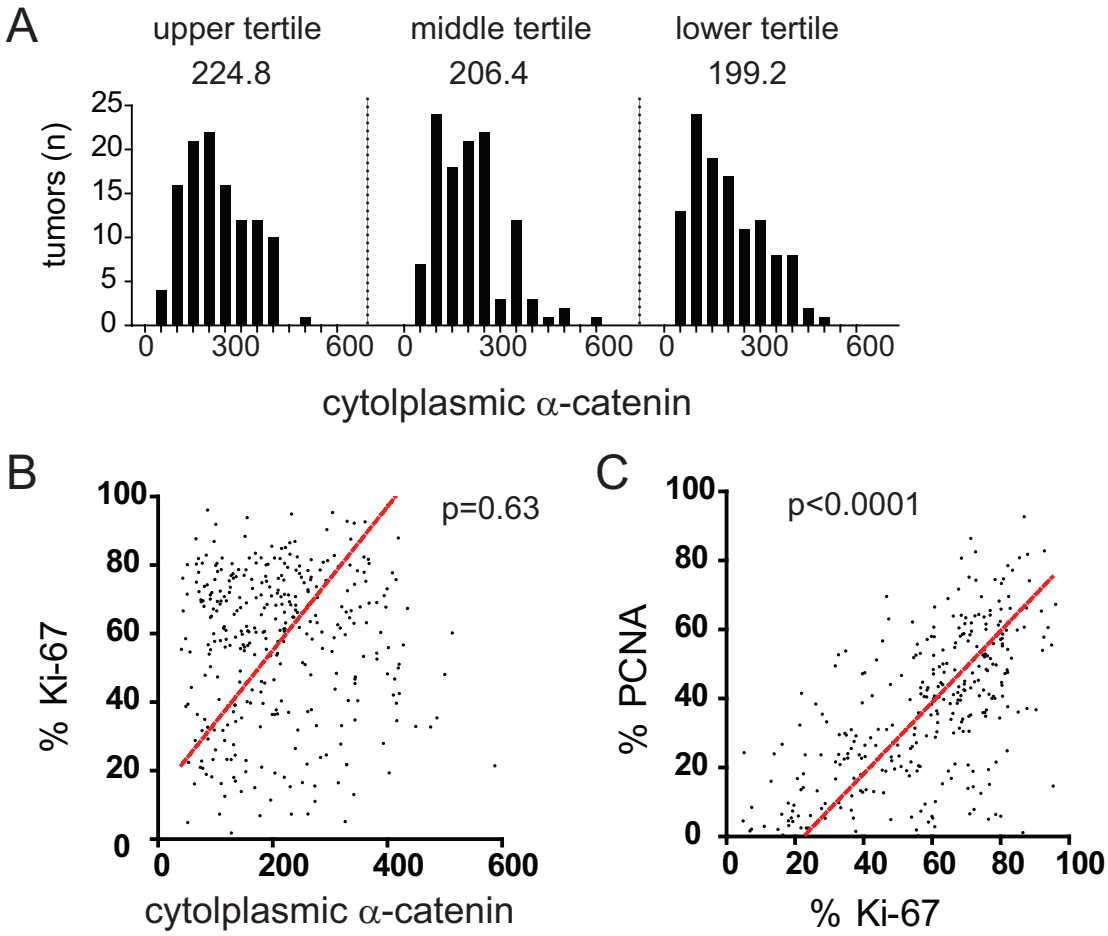

Fig. S2. Control data for tumor microarray dataset. (*A*) Bar histograms showing the distribution of α-catenin levels (binned by AQUA score) in patients stratified by nuclear ß-catenin level (Fig. S1*A*). The difference in mean α-catenin level (shown above the histograms) between tertiles is not significant by ANOVA followed by posttest for linear trend. (*B*) Deming regression of %Ki-67 and levels of cytoplasmic/membranous α-catenin (in red) resulted in a line with a slope that was not significantly different from zero. (*C*) Comparison of %Ki-67 and %PCNA by Deming regression (red line) revealed a slope of 1.035 ± 0.07615, suggesting that within this array, %Ki-67 is a valid marker of proliferation.

A

	benign nevi		melanoma	
	GDS1375	GDS1989	GDS1375	GDS1989
WNT1	0	0	0	0
WNT2	0	0	0	+++
WNT2B	0	0	0	+
WNT3	++	0	++++	++
WNT4	+++	+++	+	++
WNT5A	+++	++++	++	++++
WNT5B	0	0	0	0
WNT6	++++	+	++++	+
WNT7A	0	0	0	0
WNT7B	0	0	0	0
WNT8B	0	0	0	0
WNT10B	0	0	0	0
WNT11	0	0	0	0
WNT16	0/+	++++	0	++

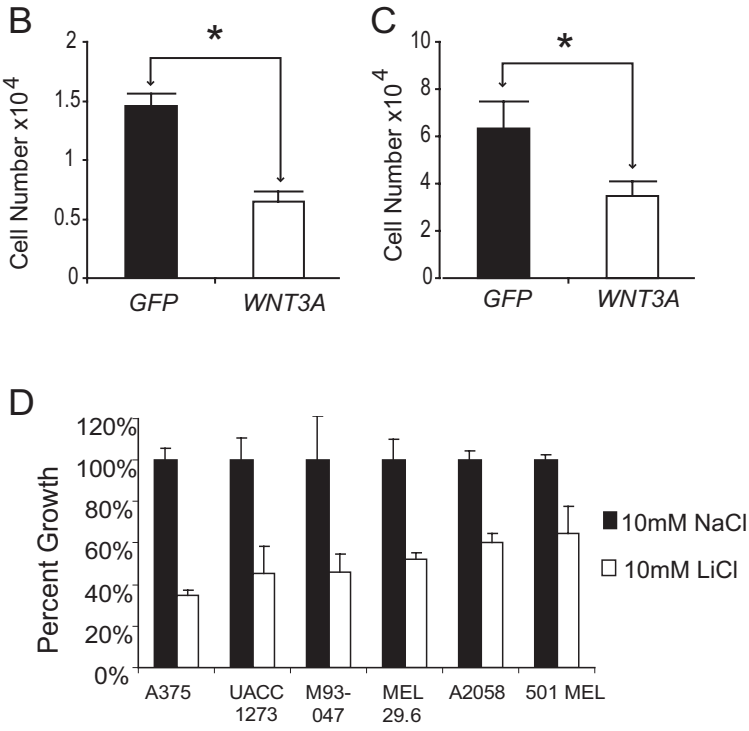

Fig. S3. WNT3A effects in human melanomas. (*A*) Data from the NCBI Gene Expression Omnibus was used to evaluate the expression of Wnt isoforms in benign nevi and melanoma tumors (see also ref. 13). The data sets used include GDS1375 (14) and GDS1989 (15). The table summarizes the data from these 2 data sets based on the reported ''detection'' call of the Affymetrix data used for all 3 data sets, and the scale indicates the percentage of samples with ''present'' calls on the expression of the different Wnt isoforms. Scoring was as follows: 0 indicates ''absent'' in all samples; + indicates expression in up to 25% of specimens; ++ indicates expression in 25%–50% of specimens; +++ indicates expression in 50%–75% of specimens; and ++++ indicates expression in 75%–100% of specimens. Few Wnt isoforms were found to be expressed by melanoma tumors based on this transcriptional profiling, and only *WNT3, WNT4, WNT5A*, and *WNT6* were detected in melanomas from both gene data sets. (*B*, *C*) The human melanoma cell lines Mel375 (*B*) and UACC1273 (*C*) were transduced with lentiviral constructs for encoding either *GFP* or *WNT3A*. Cells were counted after 3–7 days by hematocytometry; the panels shown here are representative of multiple experiments with similar results. Bars represent the average and standard deviation from 3 biological replicates. *P* values for 2-tailed *t*-tests were statistically significant (*$P < 0.05$). Expression of *WNT3A* also led to a consistent and reproducible decrease in proliferation by the MTT assay (data not shown). No consistent effect on proliferation was seen with *WNT5A* expression, again similar to the B16 cell lines (data not shown). (*D*) Human melanoma cell lines were cultured for 3–7 days in the presence of either 10 mM sodium chloride or 10 mM lithium chloride. Proliferation was measured by hematocytometry or MTT assay, and normalized to growth observed in the samples cultured in 10 mM sodium chloride. Lithium chloride inhibited proliferation in all human melanoma cell lines tested.

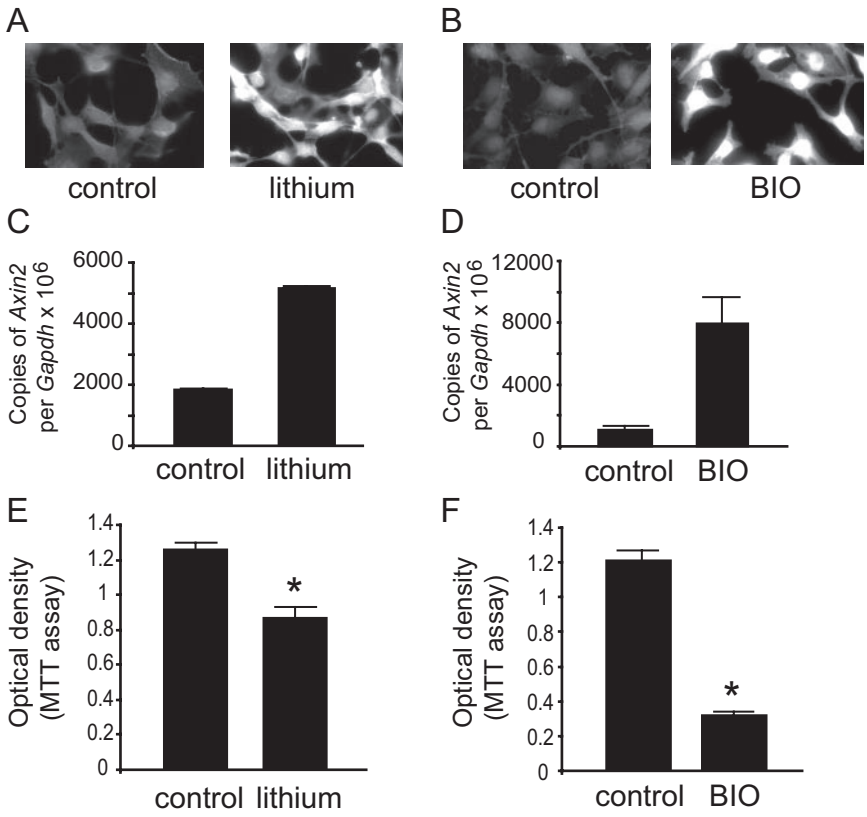

Fig. S4. Pharmacologic inhibition of *GSK3* mimics the effects of *WNT3A* on proliferation.(*A*, *B*) Immunofluorescent staining of ß-catenin demonstrated increased nuclear ß-catenin expression in B16 cells treated with 10 mM lithium chloride (*A*) or 1 μM BIO (*B*) compared with control cells treated with 10 mM sodium chloride or an equal volume of DMSO, respectively, consistent with activation of the Wnt/ß-catenin pathway by lithium chloride and BIO. (*C*, *D*) qRT-PCR demonstrated increased *Axin2* levels in B16 cells treated with 10 mM lithium chloride (*C*) or 1 μM BIO (*D*) compared with control cells, also consistent with activation of the Wnt/ß-catenin pathway by both drugs. (*E*, *F*) Representative MTT proliferation assays demonstrated decreased proliferation in B16 cells treated with 10 mM lithium chloride (*E*) or 1 μM BIO (*F*) compared with control cells. Bars represent the mean and standard deviation of 3–6 biological replicates. The difference is extremely significant by unpaired 2-tailed *t*-tests ($P < 0.001$).

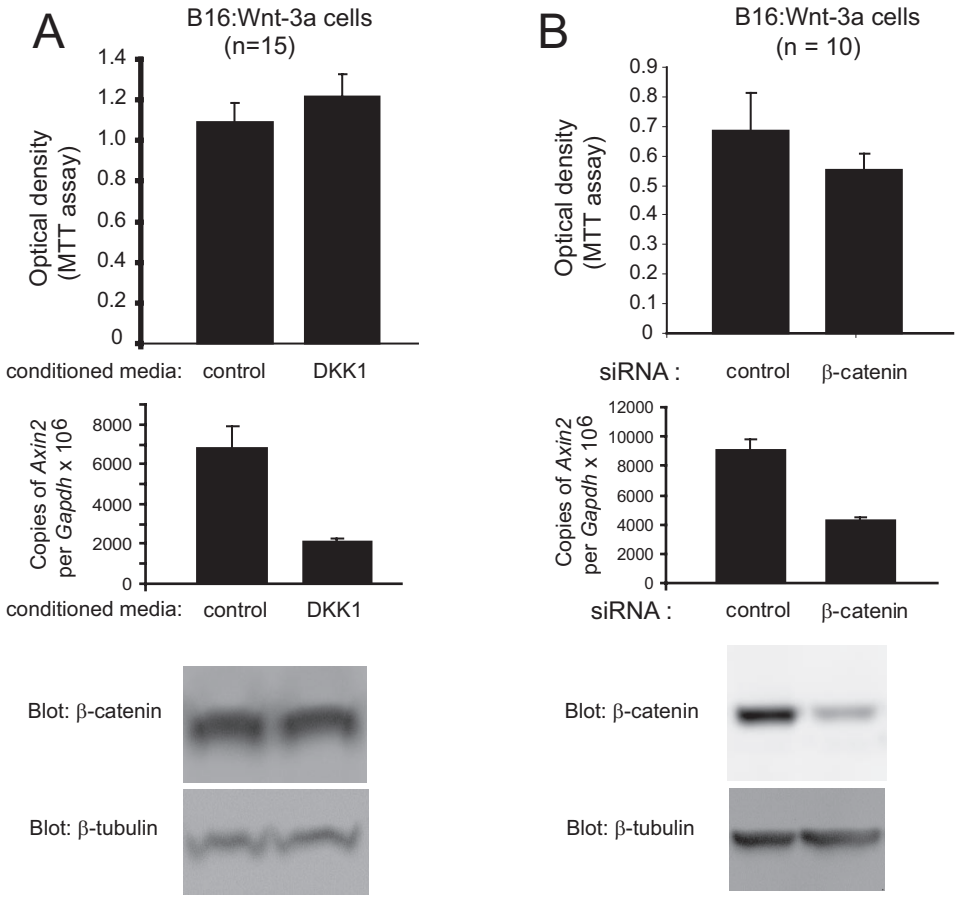

Fig. S5. Wnt/ß-catenin inhibition does not appreciably restore proliferation to B16:WNT3A cells. (*A*) B16:*WNT3A* cells were treated for 4 days with either control CM or CM containing the secreted Wnt inhibitor DKK1. Proliferation by the MTT assay (*Upper panel*) was not significantly reversed. qRT-PCR of *Axin2* confirmed inhibition of Wnt/ß-catenin signaling (*Middle panels*), whereas immunoblot analyses demonstrated no change in cellular levels of ß-catenin (*Lower panels*). (*B*) B16:*WNT3A* cells were transfected with either control siRNA or siRNA targeting ß-catenin for 3 days, after which proliferation was measured by the MTT assay (*Upper panel*). *Axin2* levels measured by qRT-PCR confirmed inhibition of Wnt/ß-catenin signaling (*Middle panels*), whereas immunoblot analyses confirmed knockdown of cellular ß-catenin by the targeted siRNA. We speculate that the differences in proliferation seen with DKK1 compared with ß-catenin siRNA are related to changes in cellular adhesion with ß-catenin siRNA that did not occur with DKK1, where cellular ß-catenin levels remained unchanged.

Other Supporting Information

Dataset S1 (XLS)